ELSEVIER

Neurocomputing

NEUROCOMPUTING

www.elsevier.com/locate/neucom

The Role of NMDA Currents in State Transitions of the Medium Spiny Neuron in a Network Model of the Nucleus Accumbens

John A. Wolf*, Jason T. Moyer, Leif H. Finkel

Departments of Neuroscience and Bioengineering, University of Pennsylvania, Philadelphia, PA, USA

Abstract

The Nucleus Accumbens (NAcb) integrates information from a wide range of glutamatergic afferent inputs, including the prefrontal cortex, hippocampus and amygdala. One of the glutamatergic receptors, the NMDA channel, has been implicated in the non-linearity of the current-voltage relationship in these cells under certain input conditions. In order to examine the relationship of the different glutamatergic receptors to the membrane response, we modeled the AMPA, GABA and NMDA receptors in the Medium Spiny (MSP) cells and their afferent input. The model demonstrates that the NMDA current is capable of sustaining certain membrane states and contributes to the non-linearity of the membrane response to input.

Keywords: Nucleus Accumbens, Striatum, NMDA, Bistability, MSP

1. Introduction

The Nucleus Accumbens (NAcb) integrates afferent information from the prefrontal cortex, hippocampus, and amygdala, and its primary output is to the ventral pallidum. [1] Due to its privileged location receiving information from many of the cognitive areas of the brain, and the high level of dopaminergic innervation from the ventral tegmental area, the NAcb has been implicated in motivational behavior and addiction. [2] Dysfunction of information processing in this area has been hypothesized to underlie aspects of schizophrenia as well. [3] Due to the probable involvement of a dysfunction of glutamatergic signaling in schizophrenia, we chose to examine the role of the NMDA receptor in the

behavior of the membrane in a multi-compartment model of the main cell in the NAcb, the MSP cell. [4]

2. The Model

The medium spiny neuron was created in the NEURON simulation environment using a 29-compartment model. [5] Appropriate channels were included from the available literature, including two sodium currents, four types of K+ currents, and six Ca^{2+} channels, and the conductances were tuned to intracellular recordings. Synaptic inputs from the prefrontal cortex were simulated using a Poisson-distributed train of inputs from a network of 100 artificial cells. Feedforward inhibition was modeled using 3 integrate-and –fire cells that received the same "cortical" inputs, but had GABAergic projections to the soma of the MSP cell (Fig.1) Up- and down-state transitions were induced by increasing and decreasing the amount of synaptic input to the cell by 2-5 times the basal level.

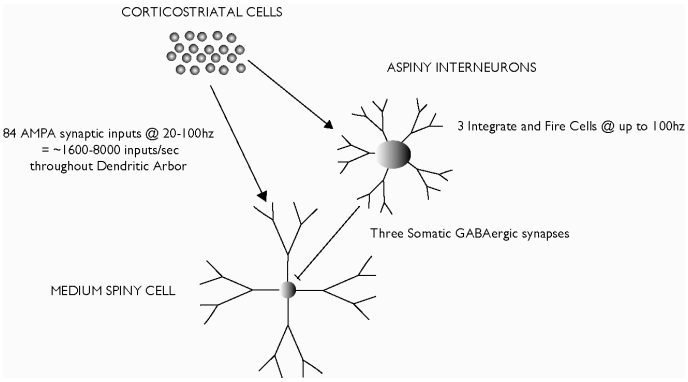

Fig.1. – Depiction of the network utilized for the simulation. Excitatory Poisson trains were fed into a 29-compartment MSP cell model and three integrate-and-fire cells that subsequently inhibit the MSP cell.

Sodium and potassium currents were modeled according to Equation 1:

$$I_z = \overline{g_z} m^x h^y \left(V_m - E_z\right). \quad (1)$$

Here, $\overline{g_z}$ and E_z represent maximum conductance and reversal potential of ion species z, respectively, and V_m is the membrane voltage of the cell. The parameters m and h are modeled according to the Hodgkin-Huxley formulation,

$$m' = \frac{m_\infty\left(V_m\right) - m}{\tau_m\left(V_m\right)}, \quad h' = \frac{h_\infty\left(V_m\right) - h}{\tau_h\left(V_m\right)}. \quad (2)$$

In this formulation, m represents the activation state of the channel, h represents the inactivation state of the channel, and m_∞, h_∞, τ_m, and τ_h are the steady state-activation curves and time constants for m and h.

Calcium channels were modeled using the Goldman-Hodgkin-Katz equation, which accounts for current rectification at elevated membrane potentials:

$$I_{Ca} = P_{Ca} z^2 \frac{V_m F^2}{RT} \frac{\left[Ca^{2+}\right]_i - \left[Ca^{2+}\right]_o \exp\left(-zFV_m/RT\right)}{1-\exp\left(-zFV_m/RT\right)}. \qquad (3)$$

Here, Pca is channel permeability to calcium ions, z is calcium valency, F is Faraday's constant, R is Boltzmann's constant, T is temperature, and $\left[Ca^{2+}\right]$ is intracellular or extracellular calcium concentration.

GABA and AMPA currents were modeled using a two-state synapse provided in the standard NEURON package, with rise and decay time constants adjusted as in Table 1. [6] The NMDA current was a modified version of the NMDA receptor described in [7] and available from SenseLab (senselab.yale.med.edu). In this channel, current is defined as

$$I_{NMDA} = \overline{g_{NMDA}}\, R\, B\left(V_m\right)\left(V_m - E_{NMDA}\right), \text{ with} \qquad (4)$$

$$B\left(V_m\right) = \frac{1}{1+\frac{\left[Mg^{2+}\right]_o}{3.57mM}\exp\left(-V_m \cdot 0.062mV^{-1}\right)}. \qquad (5)$$

In this case, $B\left(V_m\right)$ represents voltage-dependent magnesium blockade [8], $\left[Mg^{2+}\right]_o$ is the extracellular magnesium concentration, and R is described by a two-state kinetic scheme. Parameter values for GABA, AMPA, and NMDA currents are listed in Table 1; note that τ_{on} and τ_{off} are the time constants describing rising and decaying phases of the current, respectively, while $\overline{g_z}$ is the maximum conductance for a single channel. $\overline{g_z}$ was found by adjusting the single-channel current to approximate whole-cell current when multiplied by the number of synapses, i.e:

$$I_{NMDA,Single\,Channel} = \frac{I_{NMDA,Whole\,cell}}{N_{NMDA,Whole\,cell}}, \qquad (6)$$

where N_z is the number of channels in the cell.

Table 1. Synaptic current parameters for the MSP cell model.

Current	$\overline{g_z}(nS)$	$E_z(mV)$	N_z	$\left[Mg^{2+}\right]_o$	$\tau_{on}(ms)$	$\tau_{off}(ms)$	Location
NMDA	0.13	0	84	0.1	40.0	298.9	Dend
AMPA	0.03	0	84	–	2.2	11.5	Dend
GABA	0.03	-60	3	–	1	5.5	Soma

3. Results

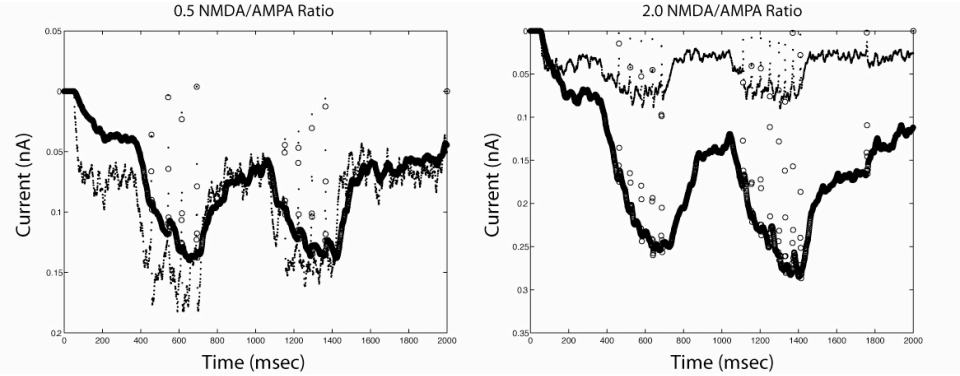

Fig.2. – Levels of Whole Cell AMPA (dots) and NMDA (circles) current throughout the 2 seconds of the simulation. Whole cell currents are shown from an NMDA/AMPA level of 0.5 and 2.0.

The model reproduced up and down state transitions of the MSP cell when inputs were less than one-half of those used to generate the up state. There were no spontaneous changes between states other than those driven by input changes.

The NMDA to AMPA ratio was adjusted from 0.5 to 2 at 0.5 increments in order to evaluate what effect this has on state transitions of the membrane potential. There was a significant change in measurable whole cell current through the NMDA receptors when the current ratio was adjusted. (Fig.2)

The increase in current through the NMDA channels led to a number of effects. There were significantly more spikes in the up state, and the overall average membrane potential increased. At higher levels of NMDA/AMPA ratios there was a tendency for the membrane to stay in the “up” state, and even for spikes to appear between “up” states when there was previously a “down” state transition. (Fig. 3). Increasing L-type conductance to ten times the conductance reported in the literature did not affect transitions between the up and down states of the cell.

4. Conclusions

The model reproduces the changes in state brought about by shifts in the number of inputs. The influence of the NMDA currents on these transitions and its contribution to the higher membrane state of the MSP cell has been discussed in the literature. [9] The model confirms that at realistic levels of NMDA current, this current can indeed sustain the MSP cell in a higher voltage state, even after the number of inputs has decreased. The ratio of NMDA/AMPA in these cells is crucial to determining the effect of the NMDA current in the model, and has been demonstrated to change after cocaine treatment in rats.[10] In the model, the total current was kept constant, and this ratio was changed. Due to the longer time constant of the NMDA current, this current continues to flow after

the period of firing that caused the up-state is over. While it has been proposed that the L-type current interacts with the NMDA current to keep cells in the up state, we were unable to reproduce this with ten times the known Ca^{2+} current in these cells. This could be due to changes in the kinetics of the L-type currents in the striatum that are not modeled here, and is currently under investigation.

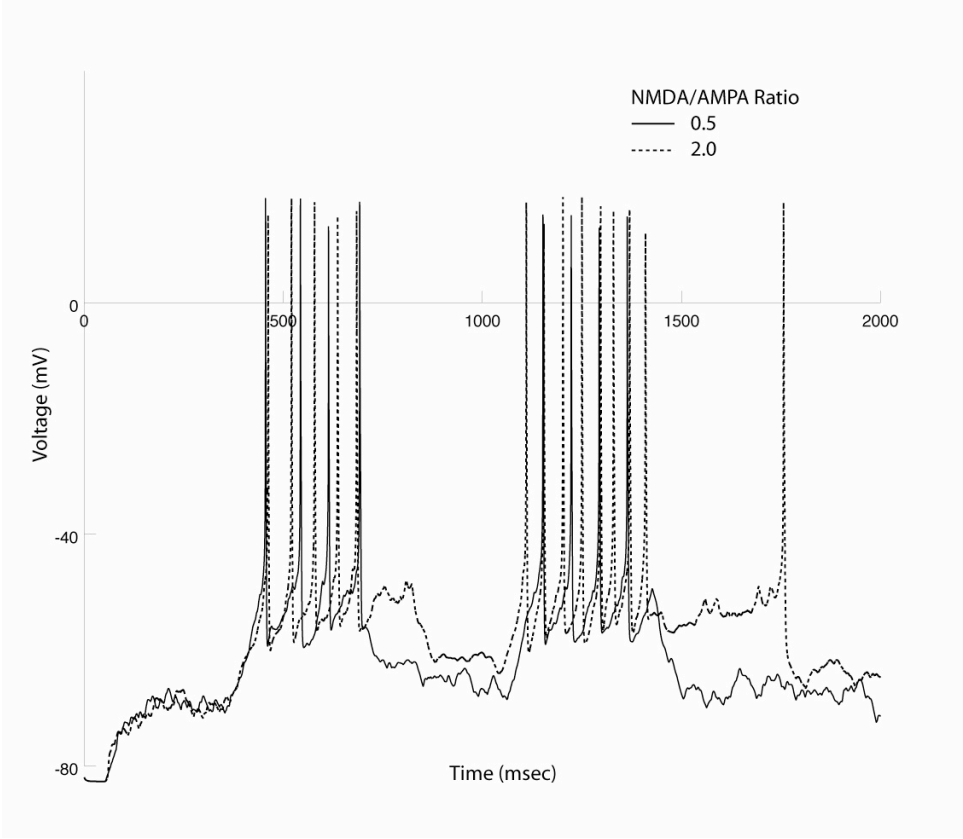

Fig. 3. Voltage traces from the MSP model showing representative traces from simulation runs with different NMDA/AMPA ratios. Note the increased time in the up state of the cell and the increase in the number of spikes with the NMDA/AMPA ratio of 2.

The NMDA receptor is involved in the induction of LTP, which has been discussed as a possible substrate for memory formation. The accumbens has also been implicated in reward-related learning and motivated behavior. [11] The NMDA receptor is a coincidence detector that will open only if glutamate is bound and the voltage levels are appropriate due to the Mg^{2+} block. It has been proposed that Ca^{2+} entering through these channels leads to an increase in AMPA receptor insertion and therefore strengthening the synapse. [12] If the NMDA/AMPA current ratio is involved in keeping the cell in the up state, learning could enhance the output of those MSP cells involved in the behavior. Since there is a large feedback loop in the cortico-accumbens circuit, this mechanism may be involved in learning of motivated behavior.

Acknowledgements

The authors would like to thank Ashlan Reid for assistance with the code for the NMDA channel, and Maciej Lazarewicz for helpful discussion. This work was supported by an NIH MH-064045 Conte Center grant.

References

[1] Zahm DS. An integrative neuroanatomical perspective on some subcortical substrates of adaptive responding with emphasis on the nucleus accumbens. Neurosci Biobehav Rev 2000;24(1):85-105.

[2] Pennartz CM, Groenewegen HJ, Lopes da Silva FH. The nucleus accumbens as a complex of functionally distinct neuronal ensembles: an integration of behavioural, electrophysiological and anatomical data. Prog Neurobiol 1994;42(6):719-61.

[3] Grace AA. Gating of information flow within the limbic system and the pathophysiology of schizophrenia. Brain Res Brain Res Rev 2000;31(2-3):330-41.

[4] Moghaddam B. Bringing order to the glutamate chaos in schizophrenia. Neuron 2003;40(5):881-4.

[5] Hines ML, Carnevale NT. The NEURON simulation environment. Neural Comput 1997;9(6):1179-209.

[6] Gotz T, Kraushaar U, Geiger J, Lubke J, Berger T, Jonas P. Functional properties of AMPA and NMDA receptors expressed in identified types of basal ganglia neurons. J Neurosci 1997;17(1):204-15.

[7] Destexhe A, Mainen ZF, Sejnowski TJ. Synthesis of models for excitable membranes, synaptic transmission and neuromodulation using a common kinetic formalism. J Comput Neurosci 1994;1(3):195-230.

[8] Jahr CE, Stevens CF. A quantitative description of NMDA receptor-channel kinetic behavior. J Neurosci 1990;10(6):1830-7.

[9] Vergara R, Rick C, Hernandez-Lopez S, Laville JA, Guzman JN, Galarraga E, Surmeier DJ, Bargas J. Spontaneous voltage oscillations in striatal projection neurons in a rat corticostriatal slice. J Physiol 2003;553(Pt 1):169-82.

[10] Thomas MJ, Beurrier C, Bonci A, Malenka RC. Long-term depression in the nucleus accumbens: a neural correlate of behavioral sensitization to cocaine. Nat Neurosci 2001;4(12):1217-23.

[11] Cardinal RN, Parkinson JA, Hall J, Everitt BJ. Emotion and motivation: the role of the amygdala, ventral striatum, and prefrontal cortex. Neurosci Biobehav Rev 2002;26(3):321-52.

[12] Luscher C, Frerking M. Restless AMPA receptors: implications for synaptic transmission and plasticity. Trends Neurosci 2001;24(11):665-70.